

September 2005

Spatial and Temporal Variations in Epikarst Storage and Flow in South Central Kentucky's Pennyroyal Plateau Sinkhole Plain

Chris Groves

Western Kentucky University, chris.groves@wku.edu

Carl Bolster

Joe Meiman

Follow this and additional works at: http://digitalcommons.wku.edu/geog_fac_pub



Part of the [Geology Commons](#), [Geomorphology Commons](#), and the [Hydrology Commons](#)

Recommended Repository Citation

Groves, Chris; Bolster, Carl; and Meiman, Joe. (2005). Spatial and Temporal Variations in Epikarst Storage and Flow in South Central Kentucky's Pennyroyal Plateau Sinkhole Plain. *U.S. Geological Survey Karst Interest Group Proceedings*, 64-73.

Available at: http://digitalcommons.wku.edu/geog_fac_pub/28

Spatial and Temporal Variations in Epikarst Storage and Flow in South Central Kentucky's Pennyroyal Plateau Sinkhole Plain

By Chris Groves¹, Carl Bolster², and Joe Meiman³

¹Hoffman Environmental Research Institute, Western Kentucky University, Bowling Green KY 42101

²USDA ARS Animal Waste Management Research Unit, Bowling Green KY 42104

³Division of Science and Resource Management, Mammoth Cave National Park, Mammoth Cave, KY 42259

ABSTRACT

The well-developed karst aquifers of south central Kentucky's Pennyroyal Plateau are impacted by contamination from animal waste and other agricultural inputs. Understanding fate and transport of these and other contaminants first requires knowledge of flow and storage behaviors within the impacted aquifers, complicated by significant heterogeneity, anisotropy, and rapid temporal variations. Here we report on spatial and temporal variations in vadose zone flow and water chemistry (or quality) within Cave Spring Caverns, Kentucky beneath agricultural lands on a well-developed sinkhole plain. Weekly sampling of three underground waterfalls show statistically significant differences in water quality, though the sites are laterally within 160 m and are all located about 25 m underground, in a groundwater basin of about 315 km². These reflect a combination of differences in epikarst flow and land use above the cave. High-resolution (minutes) monitoring of precipitation recharge along with flow and specific conductance in one of the waterfalls reveals a significant storage and mixing reservoir within the soil/epikarst zone. Varying precipitation rates and antecedent moisture conditions result in a range of storm responses observed at the waterfall, depending in part on whether this reservoir is filled or depleted. Slow and rapid flow paths through this storage zone were observed, the latter triggered by high recharge rates. These observations are generally consistent with the interpretations of Perrin and others (2003) from a Swiss limestone aquifer in a somewhat different hydrogeologic setting, strengthening the idea that epikarst and, more generally, vadose zone storage play a key role influencing flow and transport within karst aquifer systems.

INTRODUCTION

Well-developed karst aquifers are extremely vulnerable to contamination due to the ease and rapidity with which fluids can enter and move through these systems. For example, within south central Kentucky's Pennyroyal Plateau, contamination of groundwater by agricultural contaminants associated with animal waste such as fecal bacteria and nitrate is widespread (Currans, 2002; Conrad and others, 1999). Understanding agricultural impacts on karst aquifers is particularly challenging due to significant heterogeneity and anisotropy typically found in these systems, which can lead to large spatial and temporal variations in flow and water chemistry conditions.

The *epikarstic*, or *subcutaneous* zone (Williams, 1983; Perrin and others, 2003; Jones and others, 2003) forms an important component of many karst flow systems. The typically perched epikarst aquifer forms in the vicinity of the soil/bedrock interface where fractures have been widened from dissolution by acidic soil water. As the infiltrating water quickly approaches equilibrium with respect to the limestone bedrock, dissolution rates drop, as does solutionally-enhanced permeability. As a result the epikarst constitutes a relatively high permeability zone in comparison with less permeable rocks below. Evaluating the impacts of epikarst flow and storage is critical for understanding the fate and transport of agricultural contaminants within karst aquifers.

Recently progress has been made in understanding the details of karst flow and geochemical processes by high-resolution monitoring with electronic probes and digital data loggers (e.g. Baker and Brunson, 2003; Charleton, 2003; Groves and Meiman, 2005; Liu and others, 2004). The importance for understanding karst dynamics comes not as much for the ability to automatically collect data in relatively remote locations, as for the ability to collect high temporal resolution data. Flow and chemical data with a resolution of minutes capture all significant structures of hydrologic variation, even for karst systems. This can be useful for interpreting information about aquifer structure by comparing the detailed timing and magnitudes of related phenomena. In a recent example, Liu and others (2004) interpreted controls on aquifer behavior in southwest China's tower karst by comparing rates, directions, and magnitudes of changes in water levels, specific conductance (spC), saturation indices, and PCO_2 in storm responses from a large karst spring and nearby well.

While the long-term goal of the research we describe here is to quantitatively understand fundamental controls on relationships between agricultural land use and karst groundwater quality, here we evaluate epikarst flow and storage within south central Kentucky's Pennyroyal Plateau sinkhole plain based on vadose water sampling from three waterfalls located beneath active farming land. Evaluating the hydrologic behavior of the epikarst at the site is a critical step to quantitatively evaluating the fate and transport of agricultural contaminants.

FIELD SITE

Three subsurface waterfalls are being monitored, as well as rainfall and other atmospheric parameters, within and above Cave Spring Caverns (Figures 1-4) near Smiths Grove, Kentucky. The cave is located beneath a small portion of the extensive sinkhole plain of the Pennyroyal Plateau within the Mississippian Plateaus Section of the Interior Low Plateaus Physiographic Province. Just over 2 km of large horizontal cave passages pass beneath several farm fields, with the cave floor typically

about 25 m below the ground surface. Water enters at numerous locations as perennial or intermittent streams or waterfalls. The recharge area lies within the Graham Springs Groundwater Basin (Ray and Currens, 1998) which discharges at Wilkins Bluehole on the Barren River, 18 km to the southwest. Wilkins Bluehole is the second largest spring in Kentucky, with a minimum discharge of $0.56 \text{ m}^3/\text{s}$ (Ray and Blair, in press).

The cave is formed within the upper part of the Mississippian St. Louis Limestone (Richards, 1964). The Lost River Chert, a discontinuous unit of silica-replaced limestone typically 2-3 m thick near the site, lies between the ground surface and the cave. Locally, beds dip gently to the west at about $1-2^\circ$.

South central Kentucky has a humid-subtropical climate. Using climatic data from the Mammoth Cave and Bowling Green areas, Hess (1974) estimated that the area has a mean precipitation of 1,264 mm/yr, and the mean-annual temperature is 13°C . Late summer and early fall are drier than other months. Hess (1974) estimated that mean-annual potential evaporation is 800 mm, varying from near zero to over 100 mm/mo.

The three percolation waterfalls--1, 2, and 3 in order moving into the cave--fall between about 5 and 8 m from the ceiling along the east side of the main passage starting about 40 m north of the cave's entrance, within a 160 m section of the passage (Figure 1).

METHODS

There are three related sampling programs: surface weather conditions, weekly sampling and laboratory analysis of water at the three waterfalls, and 2-minute monitoring of flow, specific conductance (spC), pH, and temperature at waterfall 1. Details of these sampling programs are provided as follows:

Surface Rainfall

On the surface 110 m south of the cave entrance is an automated HOBOTM weather station that collects rainfall, temperature, wind speed and direction,

relative humidity, and solar radiation (Figure 2). Rainfall is resolved to the nearest 0.25 mm, and summed every five minutes. Due to interference by birds over part of the reported period, we utilized five-minute rainfall after 25 March 2005 (including storms 2, 3, and 4 discussed below) from the National Park Service Atmospheric Monitoring Station near the town of Pig, 9.5 km to the northeast.

Field Collection and Laboratory Analysis

Water was collected from each waterfall weekly in sterile, acid-washed HDPE bottles and stored on ice. In most cases water was analyzed within three hours of collection. Water samples were analyzed for a suite of parameters indicative of limestone weathering (e.g. Ca, Mg, alkalinity, and specific conductance (spC)) and agricultural impact (e.g., NO_3 , PO_4 , and NH_4). Alkalinity was measured using the inflection point titration method (Rounds and Wilde, 2001) and reported as mg/L CaCO_3 mg/L. Ca and Mg were analyzed in triplicate using inductively coupled plasma optical emission spectroscopy (ICP-OES). NO_3 , PO_4 , and NH_4 were measured in triplicate using a Lachat "QuickChem" method. Preliminary analysis indicated that particulate-associated Ca, Mg, and nutrients were minimal; subsequently water samples were not filtered prior to analysis. Dissolved oxygen (DO), pH and spC were measured in the field with a YSI 556 multi probe system (YSI Environmental). Data were collected from February 23, 2005 to May 25, 2005 for Ca, Mg, spC, and DO (n=13), March 3, 2005 to May 25, 2005 for alkalinity (n=12), and March 23, 2005 to May 25, 2005 for NO_3 , PO_4 , and NH_4 (n=10).

Data Logging at Waterfall One

The site is equipped with an array of electronic sensors and loggers and tied to a common tipping bucket rain gauge (Campbell Scientific (CSI) TE525) resolving tips of 0.1 mm. Discharge from the rain gauge is directed into 10-mm Tygon tubing which feeds a PVC flow-through chamber (20 mm ID) mounted with a series of three Cole-Parmer double-junction industrial in-line ATC pH sensors.

Each pH sensor is connected to a three-meter shielded coaxial cable and terminates in the instrument box (Pelican 1400) at a Cole-Parmer preamplifier to increase signal stability. This pH system can resolve pH to ± 0.01 SU. The pH flow-through chamber discharges into a section of 10-mm Tygon tubing where it is split into three paths, each passing through a CSI CS547A-L specific conductance/temperature sensor. This sensor can resolve temperature to $\pm 0.1^\circ\text{C}$ and specific conductivity to ± 0.001 mS. The three paths are then rejoined into a single section of tubing and positioned at an elevation approximately 40 cm higher than the sensors to assure pipe-full conditions. The signal from the rain gauge is split into three cables, each connected to a CSI CR10X digital micrologger (Figure 3). Each micrologger is connected to its corresponding set of pH, conductivity (spC) and temperature sensors. This redundancy in spC, temperature, pH, and data loggers not only ensures backup in the case of malfunction, but when fully operational we calculate means, standard deviations, and coefficients of variation (CV) for each observation. The 14,359 spC observations (each made in triplicate) reported in this paper had an average CV of 2.7%. This value is similar to the CV of Waterworks Spring (2%) which has been considered the only perennial "diffuse flow" spring in the region. Waterworks Spring is located near conduit dominated Wilkins Bluehole, which has a greater CV at 14% (Quinlan and others, 1983; p. 57).

Every 30 seconds the micrologger program is executed. The program is set to output tip totals from the rain gauge every five minutes, and to average the 30-second pH, spC, and temperature values every two minutes. To reduce redundant data the program compares the current two-minute average values of each sensor to that of the previous two-minute average. If the absolute value of change exceeds a preset value--the current two-minute average values for all sensors is committed to final storage. In any event, the current two-minute values are always stored once per hour. In this way we achieve two-minute resolution even during hourly recording, because we know under those static conditions the observations have not varied beyond the threshold value.

The waterfall flow data are given in tips per minute for the tipping bucket gage, but these do not yield discharge directly because some of the water, especially at higher flows, falls outside of the bucket orifice. These data thus only give a relative flow indication, but the signals (Figure 5) give a clear indication of dry and wet conditions and their correlation with rainfall events. We are in the process of developing a rating curve relating tips per minute to actual discharge, which we measure periodically by catching the flow in a large tarp and measuring the volumetric flow rate with a 10 liter bucket.

Statistical Analysis of Water Quality Data

Single-factor analysis of variance (ANOVA) was used to determine if statistically significant differences exist in important water quality parameters between the three waterfalls. Differences between waterfall locations may reflect different residence times and land use activities at the surface. Prior to analysis, Ca, NO₃, PO₄, and spC were log-transformed whereas Mg was inverse-transformed to obtain approximately normal distributions. Alkalinity, on the other hand, was normally distributed so no transformation was needed. Fisher's t-test was used to compare means between different waterfalls (Helsel and Hirsch, 1993). All statistical analyses were performed using SAS version 9.1 (SAS Institute Inc., 2003).

RESULTS

Temporal Variations at Waterfall One

Between 21 March and 10 April 2005, precipitation, waterfall flow, and spC data reflect four succeeding rain events that occurred over progressively wetter antecedent moisture conditions. Although we currently lack data for a rating curve, discharge directly measured under very dry conditions at the waterfall (31 May 2005) was 0.04 L s⁻¹. Using an empirical value of 1.98 L s⁻¹ km⁻² for unit base flow (Quinlan and Ray, 1995), derived from preliminary data for the autogenic recharge area of the Graham Springs Basin (Joe Ray, Kentucky Division of

Water, personal communication, 2005), this discharge corresponds to an estimated recharge area for the waterfall of about 2 ha. Estimates of three epikarst spring recharge areas at other sites in Kentucky range from 4-8 ha (Ray and Idstein, 2004). Although the rainfall data after 25 March (storms 2-4) are from 9.5 km away, they show close correlation to the cave signals when there was a response.

Responses of the cave parameters show a varying behavior following the different storm events and thus provide information on flow and storage within the aquifer system. Flow in the waterfall, initially under relatively dry conditions, began to increase within 2.3 hours of the onset of significant rainfall measured above the cave system, and showed a clear flow increase of about 120% that returned to the original condition within about 1.5 days. However, there was no systematic change in the spC signal following this rainfall, as explained later.

About three days later a more intense storm occurred with obvious differences in the cave response. While the timing of the flow increase was similar to the first storm (though rain data for this storm are from the NPS station), flow rates stayed more than twice as high as the initial condition for more than four days without significant rainfall, rather than returning quickly to pre-storm levels. The spC signal from relatively dilute rainfall quickly moving through the system was also clear and corresponded to rainfall intensity, reaching a low of about 160 μS cm⁻¹, or about 70% of pre-storm levels, after an intense thunderstorm cell in which rainfall intensity exceeded 5 cm hr⁻¹. We lost data on peak waterfall flow rate because the flow exceeded the limits of the tipping bucket mechanism, but later modified the equipment to accommodate higher flows.

The next storm, about four days later, was different from the first two with respect to both signals. Flow rates continued at a similarly high level without an appreciable increase, while spC dropped again in very clear relation to rainfall. In contrast to the second storm, however, spC took more than seven days to rise to the same level that had taken

only two days after the previous rainfall, even though starting at a higher minimum level.

Finally, a small storm about five days later, which began with waterfall flow rates at a similarly high rate and spC still uniformly rising through time to pre-storm three levels, had little or no impact on waterfall behavior.

Spatial Water Quality Variations

Significant variations in water quality were observed between the three waterfalls (Figure 6). Both Ca and Mg were significantly higher in waterfall 2 and this is consistent with higher alkalinity and spC values at this location. The average Ca concentration for waterfall 2 was 50.7 mg L^{-1} compared to 32.1 mg L^{-1} and 33.4 mg L^{-1} for waterfalls 1 and 3, respectively (Figure 6A). Similarly, the average concentration of Mg in waterfall 2 was 8.57 mg L^{-1} compared to 5.93 mg L^{-1} for waterfall 1 and 5.02 mg L^{-1} for waterfall 3 (Figure 6B). Alkalinity and spC were also highest in waterfall 2. Mean alkalinity for waterfall 2 was $106 \text{ mg CaCO}_3 \text{ L}^{-1}$ and for waterfalls 1 and 3 the mean concentrations were $73.3 \text{ mg CaCO}_3 \text{ L}^{-1}$ and $60.0 \text{ mg CaCO}_3 \text{ L}^{-1}$, respectively (Figure 6C). Mean spC was $328 \text{ } \mu\text{s cm}^{-1}$ for waterfall 2, $236 \text{ } \mu\text{s cm}^{-1}$ for waterfall 1, and $238 \text{ } \mu\text{s cm}^{-1}$ for waterfall 3. Differences between waterfall 2 and waterfalls 1 and 3 were statistically significant at the 99% confidence level (Figure 6D).

As was the case with Ca, Mg, spC, and alkalinity, PO_4 was significantly higher in waterfall 2 ($p < 0.001$) compared to waterfalls 1 and 3 (Figure 6E). PO_4 concentrations averaged 0.204 mg L^{-1} in waterfall 2 whereas mean concentrations were only 0.063 mg L^{-1} and 0.047 mg L^{-1} for waterfalls 1 and 3, respectively. NO_3 , on the other hand, was highest in waterfall 3 and lowest in waterfall 1 (Figure 6F). The average concentrations of $\text{NO}_3\text{-N}$ were 10.4 mg L^{-1} , 8.19 mg L^{-1} , and 5.60 mg L^{-1} for waterfalls 1, 2, and 3, respectively. (For reference, the EPA $\text{NO}_3\text{-N}$ Maximum Contaminant Level for drinking water is 10 mg L^{-1}) Statistical analysis on log-transformed $\text{NO}_3\text{-N}$ data indicated that concentrations between the three waterfalls were significantly different ($p < 0.001$). NH_4 concentrations were at or below

detection limit (0.02 mg L^{-1}) for all sampling times at each location.

DISCUSSION

Although the three waterfalls are separated laterally by a total of only about 160 m and at about the same depth underground, within a groundwater basin of over 315 km^2 (Ray and Currens, 1998), statistically significant differences occur in water chemistry between the three sites. These appear to result from a combination of different land use types and subsurface flow path conditions. Differences between parameters expected to result from dissolution of limestone, including Ca, Mg, alkalinity (closely related to bicarbonate concentrations), and spC, appear to indicate a difference in residence times for the flow paths leading to these waterfalls. Increased residence times may be due to greater flow path lengths and/or slower rates of movement through the epikarst and sections of the vadose zone below. Waterfall 2, for example (Figures 6A-6D), shows significantly higher concentrations than waterfalls 1 and 3 with respect to each of these four parameters.

The elevated concentrations of NO_3 and PO_4 measured in the waterfalls, particularly in waterfalls 2 and 3, suggest impact from agricultural land use in the cave's recharge zone. Although we currently lack data to discriminate the individual waterfall recharge zones (tracer testing is in progress to evaluate these), there are three different patterns in the concentrations of these compounds (Figures 6E and 6F) and indeed three general types of land use above the cave (Figure 1). Above and south of the first 90 m of the cave entrance (Figure 1, parcel A) is residential, the area to the north over the next 200 m (parcel B) had row crops (wheat) during the sampling period, and the area across the road to the east (parcel C) had cattle production. The row crops had both animal waste and chemical fertilizers applied before and during the study, while no chemicals were applied to either parcel A or C during or before sampling. While somewhat speculative until more data become available, a hypothesis consistent with the results so far might indicate that waterfalls 1, 2,

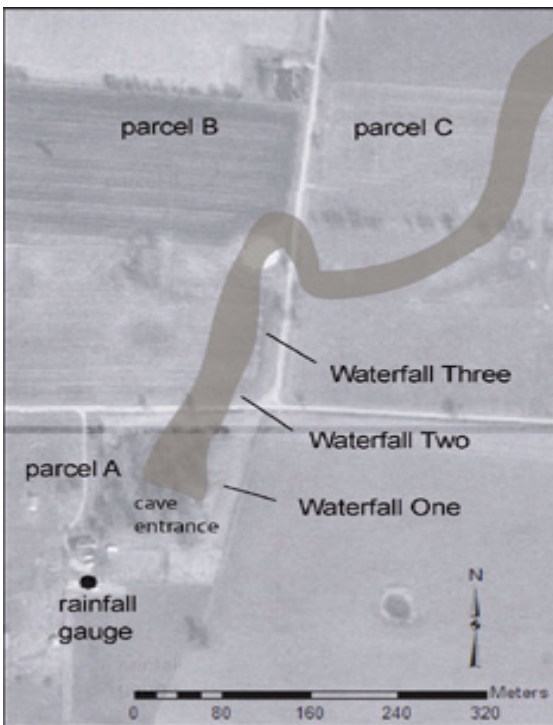


Figure 1. Map of the entrance area to Cave Spring Caverns showing sampling locations in relation to surface.



Figure 2. Weather station for recharge measurements, showing typical surface landscape above the cave system.

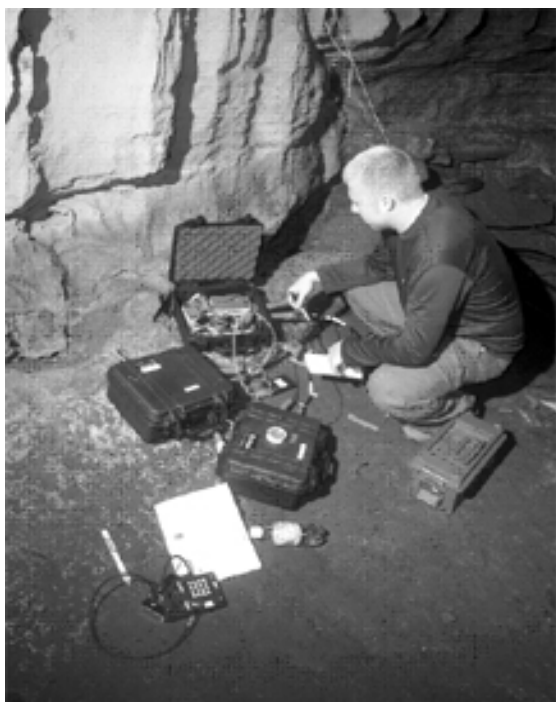


Figure 3. Triplicate Data logger system at Waterfall One.

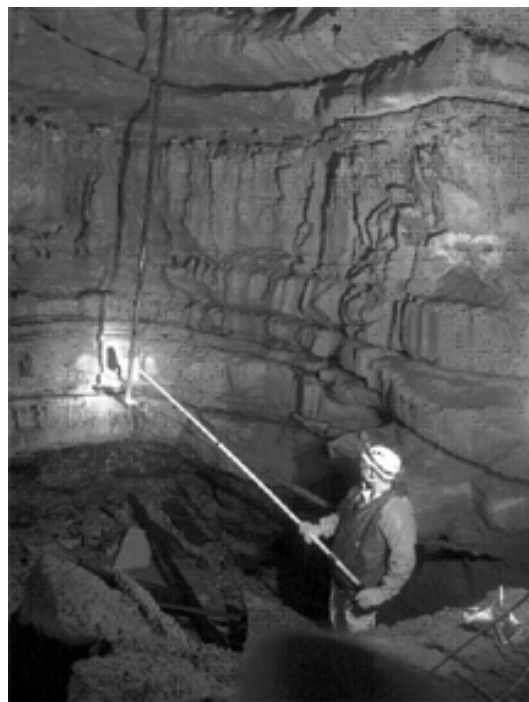


Figure 4. Water sampling at Waterfall Three using remote device to avoid a shower while sampling.

and 3 have at least partial recharge zones in parcels A, B, and C, respectively. This is indicated by water relatively low in both NO_3 and PO_4 from A (residential), higher in both from B (animal and chemical fertilizers), and from C where NO_3 is high from cattle waste but PO_4 is low because no fertilizer was applied. As the rocks within which the cave has formed are dipping to the west, it is feasible that some parts of the waterfall recharge zones could be located to the east in parcel C.

Comparison between rainfall and flow and spC at waterfall 1 (Figure 6) reveals significant storage within the soil/epikarst above the cave, as well as slow and rapid flow paths through the epikarst whose functions depend on recharge rates and antecedent moisture. The spC signal at the onset of the record ($\sim 220 \text{ mS cm}^{-1}$) represents water that has reached an approximate chemical equilibrium with the soil/epikarst system. This signal is at times diluted by rainfall that has a typical spC of 10-15 mS cm^{-1} as measured at the NPS Atmospheric Monitoring Station (Bob Carson, National Park Service, personal communication).

While the flow conditions clearly responded to the input from the first rainfall (\sim day 81) the fact that spC did not change suggests that no dilute rainwater reached the probes, and that the storm input altered the hydraulic gradients within the epikarst in a way that pushed through a slug of previously-stored water, which drained through in about 1.5 days. While another possibility is that rainwater did indeed come through quickly but had within a short period developed the chemical characteristics of the epikarst storage, consideration of later storms, discussed below, makes this unlikely.

The intense rainfall beginning on day 86 was sufficient to impact the waterfall's spC indicating a relatively rapid transport of rainwater through the system within about one-half day, although it is impossible to measure this timing more accurately as these rainfall data came from 9.5 km away. Once this flow had been established, water from a large, very intense thunderstorm cell (occurring over the cave at about the same time as the more distant rain

gauge, based on observations at the cave) caused a precipitous drop in spC within hours. While the spC returned to within 5% of its pre-storm values with less than eight hours after the spC minimum, the fact that flow remained high instead points to a significant epikarst storage reservoir. We interpret the differences in these two storms to suggest that this reservoir was relatively depleted during the dry antecedent conditions prior to the first storm, but was "replenished" during the large recharge event of storm 2. Differences in the three-dimensional head distributions within the epikarst water between the filled and depleted reservoir conditions account for differences in the responses. The more gradual return to prestorm spC conditions over the next several days reflects both mixing of storage and rainfall waters, as well as chemical reactions (limestone dissolution, for example) that increase the ionic strength of recharge water. The storm 2 response also suggests a recharge intensity threshold above which a rapid flow path is established, in addition to the more diffuse flow paths continually present.

These interpretations are consistent with the response from the third storm (day 92), which was intense but occurred under antecedent conditions with relatively full epikarst storage. The return to pre-storm chemical conditions is more gradual than in the previous storm, however, reflecting the greater proportion of storm to chemically equilibrated water within the reservoir. These two responses also indicate that the timescale for chemical mixing/ equilibration for these waters is on the order of several or more days, confirming that the slug of water pushed through during the first storm was already in the aquifer prior to that storm's onset.

Using flow and isotope measurements of rainfall and spring water, as well as underground streams leading to the spring, Perrin and others (2003) concluded that the soil/epikarst system forms an important mixing reservoir and were able to discriminate waters contributed by diffuse and rapid flow through the epikarst reservoir, the latter operating when a threshold recharge rate has been exceeded. These findings are similar to those obtained in the present study, and taken together, the

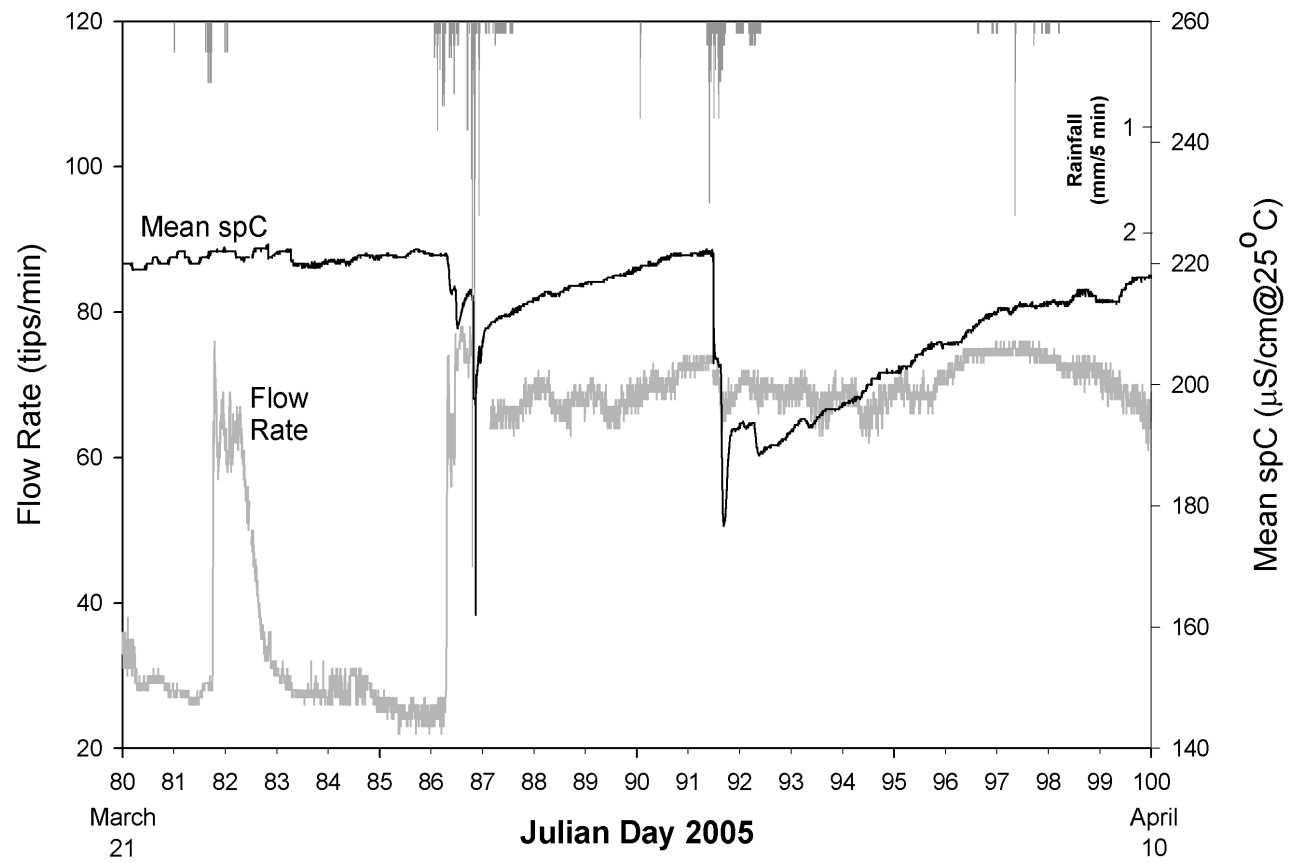


Figure 5. Plots of flow rate and mean specific conductance for waterfall 1 in Cave Spring Caverns, along with rainfall above the cave.

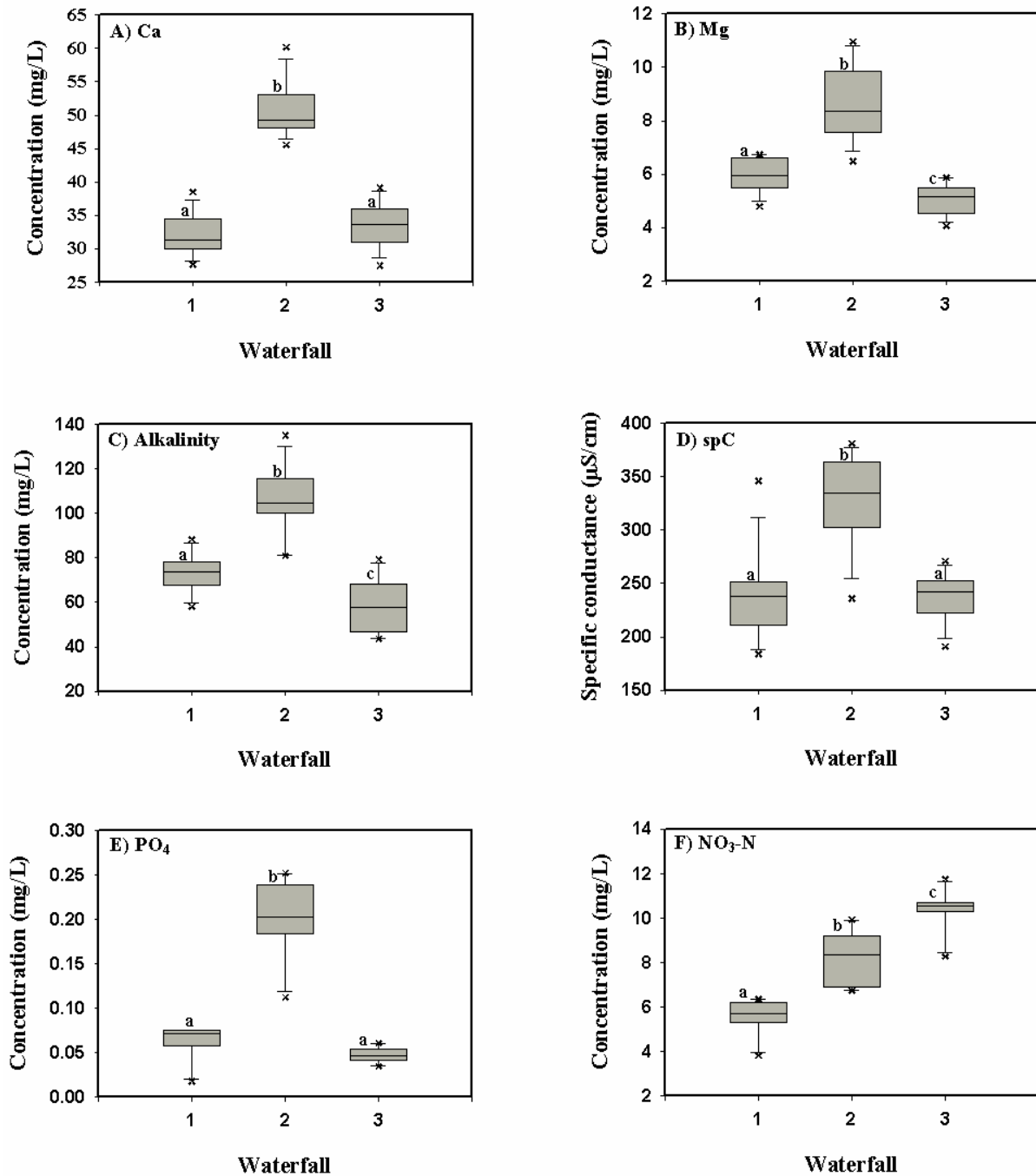


Figure 6. Boxplots of (A) calcium (mg L^{-1}), (B) magnesium (mg L^{-1}), (C) alkalinity as CaCO_3 (mg L^{-1}), (D) specific conductance ($\mu\text{S cm}^{-1}$), (E) phosphate (mg L^{-1}), and (F) nitrate-N (mg L^{-1}). boxes with same letter are not significantly different based on fisher's t-test on means of transformed (ca, Mg, Spc, NO_3 , and PO_4) and untransformed ddata (alkalinity).

two studies provide quantitative evidence to strengthen the hypothesis that vadose zone storage plays a key role influencing flow and transport within a variety of karst aquifer systems.

ACKNOWLEDGMENTS

Funding for this work was provided by the US Department of Agriculture Agricultural Research Service. We appreciate very much the kind cooperation of Bill, Linda, and Nick Marohnic for access to their land and cave, as well as the assistance of Stacy Antle, Ben Estes, Deana Groves, Pat Kambesis, Tinesha Mack, Alanna Storey, Ben Tobin, Heather Veerkamp, and Carol Wicks who provided support to the project. We also thank Joe Ray and Chuck Taylor for thoughtful reviews of this manuscript.

REFERENCES

- Baker, A. and C. Brunson, 2003, Non-linearities in drip water hydrology; an example from stump Cross Caverns, Yorkshire. *Journal of Hydrology*, v. 277, pp.151-163.
- Charleton, R.A., 2003, Towards defining a scallop dominant discharge for vadose conduits; some preliminary results. *Cave and Karst Science*. v. 30, p. 3-7.
- Conrad, P.G., D.I. Carey, J.S. Webb, J.S. Dinger, and M.J. McCourt, 1999, *Ground Water Quality in Kentucky: Nitrate-Nitrogen*. Kentucky Geological Survey Information Circular 60, Series IX, 5 p.
- Currens, J.C, 2002, Changes in groundwater quality in a conduit-flow-dominated karst aquifer, following BMP implementation. *Environmental Geology*, v. 42, p. 525-531.
- Groves, C. and J. Meiman, 2005, Weathering, geomorphic work, and karst landscape evolution in the Cave City groundwater basin, Mammoth Cave, Kentucky. *Geomorphology*, v. 67, p. 115-126.
- Helsel, D.R., and R.M. Hirsch, 1993, *Statistical methods in water resources*. Elsevier, Amsterdam, p. 529.
- Hess, J., 1974, *Hydrochemical Investigations of the central Kentucky Karst Aquifer System*. Ph.D. thesis, Department of Geosciences, The Pennsylvania State University.
- Jones, W.K., D.C. Culver, and J.S. Herman (eds.), 2004, *Epikarst*. Charles Town, WV: Karst Waters Institute, 160 p.
- Liu, Z., C. Groves, D. Yuan, and J. Meiman, 2004, South China Karst Aquifer Storm-Scale Hydrochemistry, *Ground Water*, v. 42, p. 491-499.
- Quinlan, J.F. and Ray, J.A., 1995, Normalized base-flow discharge of ground water basins: A useful parameter for estimating recharge area of springs and for recognizing drainage anomalies in karst terranes, in Beck, B.F. and Stephenson, B.F., ed., *The Engineering Geology and Hydrogeology of Karst Terranes*: Rotterdam, A.A. Balkema, p. 149-164.
- Perrin, J., P-Y. Jeannin, and F. Zwahlen, 2003, Epikarst storage in a karst aquifer: a conceptual model based on isotopic data, Milandre test site, Switzerland. *Journal of Hydrology* vol. 279, p. 106-124.
- Ray, J.A., and Idstein, P.J, 2004, Unpredictable surface exposure of epikarst springs in Kentucky, USA: in Epikarst, Jones, W.K., D.C. Culver, and J.S. Herman (eds.), Karst Waters Institute Special Publication 9, p. 140-141.
- Ray, J.A. and Currens, J.C., 1998, Mapped karst groundwater basins in the Beaver Dam 30 x 60 Minute Quadrangle, Kentucky Geological Survey.
- Richards, P.W., 1964, Geologic map of the Smiths Grove quadrangle, Kentucky. US Geological Survey Geologic Quadrangle Map GQ 357.
- Rounds, S.A., and Wilde, F.D., eds., September 2001, Alkalinity and acid neutralizing capacity (2d ed.): U.S. Geological Survey Techniques of Water-Resources Investigations, book 9, chap. A6., section 6.6.
- SAS System for Windows, version 9.1, SAS Institute Inc., Cary, NC, 2002.
- Williams, P.W., 1983, The role of the subcutaneous zone in karst hydrology. *Journal of Hydrology* v. 61, p. 45-67.